

# Magnetic and transport properties of a one dimensional frustrated t-J model for vanadate nanotubes

S. Costamagna and J. A. Riera

Instituto de Física Rosario, Consejo Nacional de Investigaciones Científicas y Técnicas,  
Universidad Nacional de Rosario, Rosario, Argentina

(Dated: March 23, 2024)

We propose a one-dimensional model consisting of a chain with a t-J Hamiltonian coupled to a Heisenberg chain in a frustrated geometry to describe the appearance of the ferromagnetic phase which has been experimentally observed in vanadate nanotubes. This model contains a mechanism of frustration suppressed by doping suggested by L. Kusun-Ebaum, et al. [Nature 431, 672 (2004)]. We study, using numerical techniques in small clusters, the relation between magnetic order and transport properties in the proposed model, and we perform a detailed comparison of the physical properties of this model with those of the ferromagnetic Kondo lattice model. For this comparison, a number of results for the latter model, obtained using the same numerical techniques, will be provided to complement those results already available in the literature. We conclude that it does not appear to be a true ferromagnetic order in the proposed model, but rather an incommensurate ferrimagnetic one, and contrary to what happens in the ferromagnetic Kondo lattice model, electronic transport is somewhat suppressed by this ferrimagnetic order.

PACS numbers: 71.10.-w, 71.27.+a, 75.30.Kz, 75.40.Mg

## I. INTRODUCTION

The possibility of taking advantage of the spin of the electrons in addition to their charge in order to develop devices with new capabilities, which is exploited in the emergent field of spintronics<sup>1</sup>, has in turn given impulse to the search for new materials with metallic ferromagnetic (FM) phases.

An extensively studied family of compounds which presents these properties is the family of the so called "manganites", for example  $\text{La}_{1-x}\text{Ca}_x\text{MnO}_3$ .<sup>2</sup> This family of manganite oxides has recently received additional interest for its property of "colossal" magnetoresistance.<sup>3</sup>

Taking into account the vast diversity of physical behavior found in transition metal oxides, it seems natural to look for this kind of properties within these materials. Following this program, it was found that a vanadium oxide ( $\text{VO}_x$ ) presents upon doping a ferromagnetic phase at room temperature.<sup>4</sup> This compound, as well as manganites,<sup>5</sup> has been synthesized as very thin cylinders or nanowires thus opening the way to their use as ferromagnetic leads in nanoscopic spin valves<sup>6,7</sup> among other devices. In this compound, double-layered nanotube "walls" of vanadium oxide are separated by dodecylammonium chains.<sup>4,8,9,10</sup> This structure is reminiscent of the carbon nanotubes which are the essential components in important devices that have already been developed.<sup>11</sup>

In manganites, it is now widely accepted that most of their relevant physical properties, particularly the property of magnetoresistance, can be explained by a single-orbital ferromagnetic Kondo lattice (FKL) model,<sup>12,13</sup> which can in turn lead to the well-known "double exchange" (DE) model in the limit of infinitely large Hund coupling. Of course, it is necessary to resort to at least a two-orbital model to describe properties related to orbital ordering.<sup>14</sup>

The purpose of the present work is to examine an alternative mechanism to the one contained in the FKL or DE models. This mechanism was suggested in Ref. 4 and is essentially based in the suppression of frustrated antiferromagnetic couplings in  $\text{VO}_x$  walls by electron or hole doping. In order to study this mechanism we propose a model inspired by the  $\text{VO}_x$  compound but we would like to emphasize that this model is not aimed at a faithful description of this material.

Our model, shown in Fig. 1 below, is a simplified one-dimensional (1D) version of the  $\text{VO}_x$  structure.<sup>8,9,10</sup> This model differs from a realistic model for  $\text{VO}_x$  not only in its dimensionality but also in a number of details such as the zig-zag geometry of the chains, the alternation between  $V_1$  and  $V_2$  along the chain, and a possible dimerization which may explain the spin gap experimentally observed in this material. Nevertheless, we believe this model will capture the essential features of the mechanism suggested in Ref. 4 and at least qualitatively some properties of the real materials. In fact,  $V_1$ - $V_2$  chains are structures present in  $\text{VO}_x$  although coupled between them in a complex way. In support of the present approach, we would like to recall that results for the one-dimensional FKL model<sup>13</sup> have reproduced many essential properties observed in manganites.

In the present manuscript we will mainly address, using numerical techniques in small clusters, the relation between magnetic order and transport properties in the proposed model, and we will perform a detailed comparison of the physical properties of the present model with those of the FKL model. For this comparison, a number of results for the latter model, obtained with the same numerical techniques, will be provided to complement those results already available in the literature.<sup>13,15,16</sup>

The paper is organized as follows. In Section II we present the model studied and we provide details of the

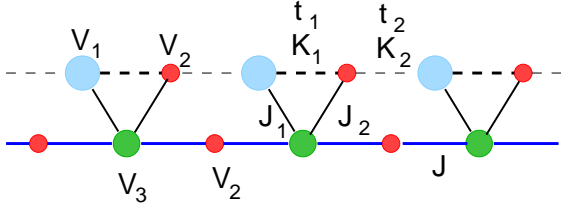


FIG. 1: A 1D model for  $\text{VO}_x$ . The upper chain, with  $V_1$  and  $V_2$  ions, is described by a t-J model, while the lower chain, with  $V_2$  and  $V_3$  ions, is described by an AF Heisenberg model.

numerical techniques employed. In Section III we show the existence of various magnetic phases in the model studied. Transport properties, in particular optical conductivity, are examined in Section IV. Section V is dedicated to emphasize differences between the present model and the FKM model.

## II. MODEL AND METHODS

The ingredients of our effective one-band model for vanadium orbitals only, which are common to  $\text{VO}_x$ , are the following (see Fig. 1). In the first place, the sites of the system correspond to three types of vanadium ions,  $V_1$ ,  $V_2$ , and  $V_3$ , with a hierarchy of hole on-site energies,  $\epsilon_1 < \epsilon_2 < \epsilon_3$ .<sup>4</sup>  $V_1$  ions are then the most likely to be occupied by holes upon doping.

The couplings between vanadium ions are mediated by oxygens and the relative values are determined by the quasipyramidal ( $V_1$ ,  $V_2$ ) and tetrahedral ( $V_3$ ) coordination between vanadium and oxygens. In the real  $\text{VO}_x$ ,  $V_1$  and  $V_2$  ions form zig-zag chains running along a given direction in one layer and in the perpendicular direction in the nearest neighbor layers. These layers of chains are connected through  $V_3$  ions which are located between them. The couplings between  $V_1$ ,  $V_2$  and  $V_3$  form a frustrated triangle of antiferromagnetic (AF) interactions.

In order to simplify the calculations we assume that double-occupancy is forbidden, which is reasonable for d-orbitals in transition metals, particularly close to half-filling. Then, the model for V-ions, with the geometry of Fig. 1 is defined by the Hamiltonian:

$$\begin{aligned}
 H = & \sum_i \epsilon_i^y c_{i+1}^\dagger c_i + H_{\text{t-J}} + \sum_i K_{i,i+1} S_i^z S_{i+1}^z \\
 & + J \sum_{\langle ij \rangle} (S_{i,2l-1} S_{j,2l-1} + S_{i,2l} S_{j,2l} + S_{i,2l+1} S_{j,2l+1}) \\
 & + \sum_i (J_1 S_{i,2l-1} S_{i,2l} + J_2 S_{i,2l} S_{i,2l+1}) \\
 & + \sum_i (1 - n_i) \quad (1)
 \end{aligned}$$

where  $c_i^\dagger$  and  $c_i$  are electron creation and annihilation

operators with the constraint of no double occupancy on  $V_1$  and  $V_2$  sites, and  $S_j$  ( $S_{s,j}$ ) are the spin-1/2 operators on the t-J (Heisenberg) chain. The first two terms correspond to the t-J Hamiltonian for the upper chain in Fig. 1, the third term to the Heisenberg Hamiltonian for the lower chain with odd (even) numbered sites corresponding to  $V_3$  ( $V_2$ ) sites, and the fourth term to the exchange couplings between these two chains. For simplicity, in the present study we will not consider dimerization in the model, and hence we adopt the hopping integrals  $t_1 = t_2 = t$  and the exchange couplings  $K_1 = K_2 = K$ , and  $J_1 = J_2$ . Besides, from the structure of  $\text{VO}_x$ , it should be  $J = J_2$  as well. All exchange couplings,  $K$  and  $J$ , are assumed antiferromagnetic.  $K = 1$  is adopted as the scale of energies.  $\epsilon_2 = 0$  gives the reference for the on-site energies;  $\epsilon_1 < 0$ , which will be a variable parameter in our study, and  $\epsilon_3 = 1$ , implying a forbidden hole occupancy on  $V_3$  sites. The  $\epsilon_3 = 1$  condition would cause localization of holes eventually occupying  $V_2$  sites on the lower chain in Fig. 1 and then it would lead to an effective cut of this chain. This is the reason why hole occupancy on  $V_2$  sites on the lower chain is forbidden in our model. In  $\text{VO}_x$ , these  $V_2$  sites would correspond to  $V_1$ - $V_2$  chains running in a perpendicular direction of the plane of Fig. 1.

At half-filling, i.e. when all sites are single occupied, the system is reduced to a frustrated spin system. In the proposed model, which could be termed a frustrated t-J (FTJ) model, charge carriers are introduced by doping with holes the t-J chain. Most of the results reported below correspond to the doping fraction  $x = 0.4$ , where  $x$  is defined as the number of doped holes divided by the number of sites of each chain,  $L$ . Although most holes would go to  $V_1$  sites in  $\text{VO}_x$ , in our model there would be a finite probability of the holes going on the  $V_2$  sites and the hopping  $V_1$ - $V_2$  would then be possible. In any case, the situation of localized holes on the  $V_1$  sites could be recovered in the  $t = 0$  limit. The inclusion of the hopping term in our model makes it more general and eventually its properties could be relevant for other compounds sharing similar structural features with  $\text{VO}_x$ . In our zero temperature study, the inclusion of this hopping is also a mimic of the activated transport that takes place in the real material.

Model (1) was studied in 2D clusters by exact diagonalization (ED), using the Lanczos algorithm, with periodic boundary conditions (PBC) and by density matrix renormalization group (DMRG)<sup>17</sup> with open boundary conditions (OBC). Using ED we were able to compute static and dynamical properties on the  $2 \times 10$  cluster, and using DMRG we studied  $2 \times 20$  and  $2 \times 40$  clusters although in this case only static properties were considered. In the results reported below obtained using the DMRG method we have retained 300-400 states in the truncation procedure.

To compute the total spin  $S$  we have adopted two procedures, (i) compute directly  $S = S(S+1)=2$ , at  $S^z = 0$  and (ii) compute  $S$  as the maximum value of  $S^z$

at which the ground state energy is recovered, which implies diagonalizing the Hamiltonian in several subspaces of fixed  $S^z$ .

Spin-spin correlations  $\langle S_j^z S_0^z \rangle$  are computed exactly with the Lanczos algorithm in the ground state, in the  $S^z = 0$  subspace. The static magnetic structure factor  $\chi(q)$  is the Fourier transform  $\chi(q) = \frac{1}{N} \sum_{i,j} \langle S_j^z S_i^z \rangle \exp(iq \cdot (r_j - r_i))$ , ( $N = 2L$ ) where  $r_j$  ( $q$ ) are the real space (reciprocal) vectors of a rectangular ladder of  $L \times 2$  sites where the lattice of Fig. 1, assuming equidistant sites, can be embedded. We have verified that the results reported below do not depend qualitatively of geometrical details (relative spatial position of the ions) of Fig. 1. Within DMRG, we measured spin-spin correlations in the  $S^z = 0$  subspace from one of the two central sites of the cluster, one belonging to the  $t$ - $J$  chain and the other to the spin chain. In this case the magnetic structure factor is computed as  $\chi(q) = \sum_j \langle S_j^z S_0^z \rangle \exp(iq \cdot j)$ , where  $0$  is one of the central sites on the spin chain and  $j$  belongs to the spin chain. In order to compare with results for the FKL model, in most of the results reported below for this model we have restricted the sum to sites on the spin chain, but they are qualitatively similar to the ones obtained with the full Fourier transform involving all sites.

A measure of the magnetic order on each chain is provided by the sum of the correlations:

$$S_H = \sum_i \langle S_{s,i}^z S_{s,0}^z \rangle \quad (2)$$

where the sum extends over the sites of the spin ( $V_3 - V_2$ ) chain and  $S_{s,0}^z$  is the spin of a  $V_3$  site on this chain.  $S_H = 0$  corresponds to an AF ordering and  $S_H > 0$  to a FM or a ferrimagnetic ordering of the spin chain.

An important property related to transport is the real part of the optical conductivity,  $\sigma(\omega) = D(\omega) + \text{reg}(\omega)$ , where  $\text{reg}(\omega)$  is defined as the spectral function:

$$\text{reg}(\omega) = \frac{1}{\omega} \sum_n \langle j_n | j_0 | \rangle^2 \delta(\omega - (E_n - E_0)) \quad (3)$$

where  $|j_n\rangle$  are eigenvectors of the Hamiltonian (1) with energies  $E_n$ , and

$$j = it \sum_i (c_{i+1}^\dagger c_i - H.c.)$$

is the current operator (in units of  $e = 1$ ) and the sum extends over the  $t$ - $J$  chain in Fig. 1.  $\text{reg}(\omega)$  was computed using the continued fraction formalism.<sup>18</sup>

From the optical conductivity, the Drude weight can be computed as:<sup>18,19</sup>

$$\frac{D}{N} = \frac{1}{N} \langle E_K - \frac{2}{\omega} \text{reg}(\omega) d(\omega) \rangle \quad (4)$$

where  $E_K$  is the kinetic energy, i.e., the negative ground state average of the hopping term of the Hamiltonian (first term in (1)).  $E_K$  is expressed in units of  $K$ , and  $D$

in units of  $e^2 K$ . As usual in the continued fraction calculation of spectral functions a Lorentzian broadening of the discrete peaks was adopted. In all the results shown below we took a Lorentzian width  $\gamma = 0.1$ .

As mentioned above, when  $J_1 = J_2 = 0$ , model (1) reduces to uncoupled  $t$ - $J$  (where  $K$  plays the role of  $J$ ) and Heisenberg chains. We are also interested in comparing our model with the FKL model with spin-1/2 localized spins defined as:

$$H = \sum_{i,j} t (c_{i+1}^\dagger c_i + H.c.) + J_H \sum_i S_i \cdot S \quad (5)$$

where  $J_H > 0$  is the Hund coupling,  $S_i$  are the localized spins and  $s_i$  are the spins of the conduction electrons. In this case the filling  $n$  is defined as the filling of the conduction chain. Notice that the  $t_{2g}$  electrons in manganese are usually modeled with spin-3/2 operators.<sup>12</sup> The frustrated  $t$ - $J$  model is perhaps more reminiscent to an extended version of model (5) which includes an AF Heisenberg exchange between localized spins.<sup>12,20,21</sup> Model (1) would also be closer to a version of the FKL model which includes a Hubbard repulsion  $U$  on the conduction orbitals,<sup>22,23</sup> since the  $t$ - $J$  Hamiltonian appears at an effective level when  $U \rightarrow \infty$ .<sup>24</sup> However, we would like to emphasize that the proposed FTJ model was not obtained from the  $U \rightarrow \infty$  limit of an underlying Hubbard-like model. In fact, most of the results reported below belong to the case of  $t = K$ .

All the results reported below correspond to the model (1) except otherwise stated.

### III. MAGNETIC PROPERTIES

We first examine the magnetic properties of this model, in particular the presence of a ferrimagnetic phase, as detected experimentally in Ref. 4. The suggested mechanism that causes this FM phase works as follows. At half-filling, due to the frustrated AF interactions, the system would be an antiferromagnet since it reduces to relatively isolated spin chains ( $V_1$ - $V_2$  chains in the real materials), or to a gapped spin liquid if these chains are dimerized. Upon electron or hole doping,  $V_1$  sites become non-magnetic, the frustration in the  $V_1$ - $V_2$ - $V_3$  triangles disappears, and the AF order in the  $V_2$ - $V_3$  subsystem of Fig. 1 implies an excess of the  $z$ -component of the total spin along one direction thus leading to ferrimagnetism or more properly, to a ferrimagnetic order.

This argument is expressed in the atomic limit. For non-zero values of  $t$ , there is a competition between the onsite energy, which tries to localize holes, and the kinetic term which tries to delocalize them. In addition, as in any  $t$ - $J$ -like model there is a competition between kinetic and magnetic energies.

Let us first examine the undoped system. Notice that by adding interactions between the  $V_2$  sites in the bottom chain of Fig. 1, and for the case  $J = K$ , one recovers

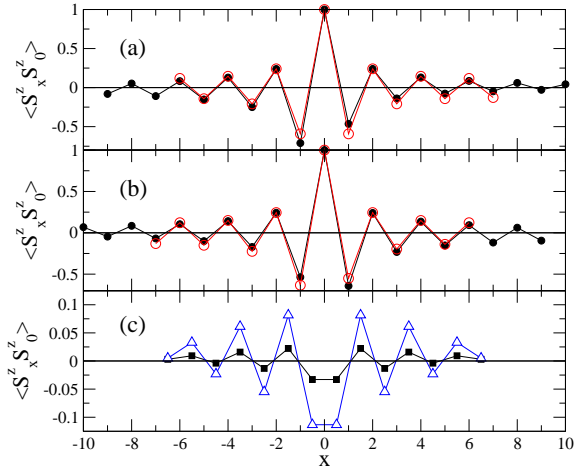


FIG. 2: (Color online) Spin-spin correlations  $\langle S_j^z S_0^z \rangle$  for the undoped system, (a) along the  $V_1$ - $V_2$  chain; (b) along the  $V_3$ - $V_2$  chain ( $V_2$  reference site). Results were obtained for the  $2 \times 14$  cluster with PBC (open circles) and for the  $2 \times 20$  cluster with OBC (filled circles),  $J=K = 0.3$ . (c) Spin-spin correlations between a  $V_3$  site and sites on the  $V_1$ - $V_2$  chain,  $2 \times 14$  cluster with PBC,  $J=K = 0.3$  (squares),  $J=K = 1.0$  (triangles). The normalization  $\langle S_0^z S_0^z \rangle = 1$  was adopted.

the frustrated AF Heisenberg ladder which has been extensively studied.<sup>25</sup> The ground state of this model is a singlet with a spin gap. If  $J < K$ , then we have an asymmetric frustrated ladder where we can expect a similar behavior. A singlet ground state could also be expected for our frustrated model. Some handwaving arguments can be put forward to support this in the case  $J < K$ . In this case, an AF order on the upper chain of Fig. 1 would dominate each frustrated triangle and the effective interactions with couplings  $J_1$  and  $J_2$  would be small. Then, both chains are essentially uncoupled and also the lower chain would present the typical AF ordering of Heisenberg chains. Our numerical calculations support this picture. In Fig. 2 we show that for both clusters with PBC and OBC,  $J=K = 0.3$ , the upper and lower chains have the spin-spin correlations  $\langle S_j^z S_0^z \rangle$  corresponding to an AF order (Fig. 2 (a) and (b) respectively). In Fig. 2 (c) we show that  $\langle S_j^z S_0^z \rangle$  between a  $V_3$  site and sites of the upper chain are indeed relatively small. In fact, we have also determined that this behavior extends up to  $J=K = 1.0$ , as shown in Fig. 2 (c). Notice the good agreement between results obtained for PBC (with exact diagonalization) and for OBC (with DMRG) where the reference site is one of the two central sites. It is worth to note that the previous argument would also imply that the undoped system is spin gapless and our numerical calculations seem to agree with this possibility.

In Fig. 3 the phase diagram of model (1) in the plane  $t; J/g$  is shown for the  $2 \times 10$  cluster and 4 holes (doping fraction  $x = 0.4$ ). For  $j_1 = 2$  (Fig. 3(a)), there is an abrupt crossover from the singlet state ( $S = 0$ ) to the ferrimagnetic state with the maximum  $S$  expected at this doping,  $S = 2$ . As  $t$  is increased the holes tend to be

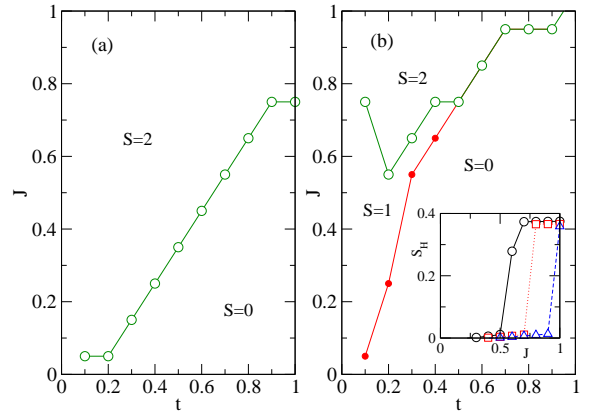


FIG. 3: (Color online) Phase diagram of model (1) on the  $2 \times 10$  cluster with 4 holes, (a)  $j_1 = 2$ , (b)  $j_1 = 1$ . The inset shows  $S_H$  (defined by Eq. (2)) for  $t = 0.3$  (circles),  $0.5$  (squares) and  $0.7$  (triangles) as a function of  $J$ .

less localized on  $V_1$  sites, and then the crossover takes place at larger values of  $J$ . When  $j_1$  is reduced, hole localization becomes less favourable, and the crossover takes place at even larger values of  $J$  for a given  $t$ , as can be seen in Fig. 3 (b), which corresponds to  $j_1 = 1$ . More interesting is the fact that, for small values of  $t$ ,  $t < 0.3$ , there is an intermediate region with  $S = 1$  between the  $S = 0$  and  $S = 2$  regions. The behavior of  $S_H$  for several values of  $t$  as a function of  $J$  is shown in the inset of Fig. 3. This quantity presents a jump at the  $S = 0 \rightarrow S = 2$  crossover, and since the nearest neighbor correlation  $\langle S_{s+1}^z S_{s,0}^z \rangle < 0$ , then there is a ferrimagnetic ordering of the spin ( $V_2$ - $V_3$ ) chain. That is, a snapshot of this system would show an alignment of the spins on the spin chain and at the same time an alignment of the spins of the  $t$ - $J$  chain with opposite orientation to the previous one.

As the cluster size is increased, the intervening regions with  $0 < S < S_{max}$  develop a "staircase", as it can be seen in Fig. 4. In Fig. 4 (a), the phase diagram in the plane  $t; J/g$  for the  $2 \times 20$  cluster, with the same doping as before,  $x = 0.4$ , is shown. These results were obtained with DMRG and the clusters have OBC along both directions. The crossovers in the phase diagram of the  $2 \times 20$  cluster were determined by comparing the energies obtained for different  $S^z$ . In this model, as well as in the FKL model discussed below, DMRG has a slow convergence and there is a tendency for low  $S^z$  subspaces to fall into metastable states. Then, in order to determine the value of  $S$  it is important to go to large  $S^z$  and then to extrapolate the difference in energy,  $E = E(S^z) - E(S^z = 0)$ , to zero. This procedure is illustrated in the inset in Fig. 4 (a). In this way we have also computed the total spin for some parameter sets, indicated in Fig. 4 (a), in the  $2 \times 40$  cluster. These values of  $S$  for the  $2 \times 20$  and  $2 \times 40$  clusters, together with the previous one for the  $2 \times 10$  cluster, seem to suggest that the ferrimagnetic phase will survive in the thermodynamically

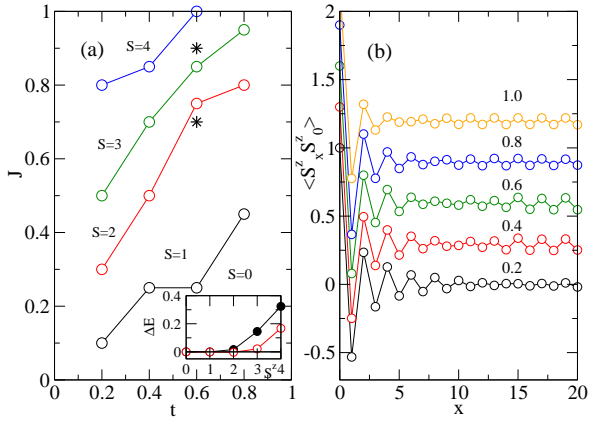


FIG. 4: (Color online) (a) Schematic phase diagram of model (1) on the  $2 \times 20$  cluster with 8 holes,  $\nu_1 = 1$ . At  $t = 0.6$ ,  $J = 0.9$  and  $0.7$  (points indicated with stars),  $S = 8$  and  $7$  respectively on the  $2 \times 40$  cluster with 16 holes,  $\nu_1 = 1$ . The inset shows  $\Delta E$  (defined in the text) vs.  $S_z$  for  $t = 0.2$ ,  $J = 0.2$  (filled symbols) and  $J = 0.4$  (open symbols),  $2 \times 20$  cluster. (b) Spin-spin correlations on the  $2 \times 40$  cluster with 16 holes,  $\nu_1 = 1$ ,  $t = 0.6$  and values of  $J$  indicated on the plot. The normalization  $\hbar^2 S_0^z S_0^z = 1$  was adopted. The curves have been shifted for the sake of clarity.

dynamic limit. It is interesting to note that we have also observed this staircase in exact diagonalization studies of the FKL model on the  $L = 10$  cluster (see below). In the suggested mechanism for ferrimagnetism, the magnetic order in the spin chain would still be an AF one. It can be seen in Fig. 4 (b) that the spin-spin correlations  $\hbar^2 S_0^z S_0^z$  for the  $2 \times 40$  clusters,  $x = 0.4$ , are indeed essentially AF except for the presence of a small kink. The same behavior was found for the  $2 \times 10$  cluster with PBC and the same doping in the  $S = 2$  region.

In order to study more systematically the behavior of the spin-spin correlations in the regions of different total spin let us turn to study the static magnetic structure factor,  $\chi(q)$ . Results for  $\chi(q)$  in the  $S^z = 0$  subspace along a "cut" at  $t = 0.8$  in Fig. 3 (a), and at  $t = 0.2$  in Fig. 3 (b) are depicted in Fig. 5 (a) and (b) respectively. These results were obtained by exact diagonalization and the first definition of  $\chi(q)$  discussed in Section II was adopted. In both cases considered, in the  $S = 0$  region (small values of  $J=K$ ),  $\chi(q)$  is maximum at  $q_x = 0$  (x is along the chain direction), indicating an AF order, irrespective of  $q_y = 0$  and  $q_z = 0$ . In Fig. 5 (a), in the  $S = 2$  region ( $J=K = 0.7$ ), the peak of  $\chi(q)$  shifts away from  $q_x = 0$ , indicating an incommensurate (IC) order. In Fig. 5 (b),  $\chi(q; 0)$  has a sudden drop upon entering in the  $S = 1$  region ( $J=K = 0.3$ ) while  $\chi(q; 5; 0)$  and  $\chi(q; 4; 5; 0)$  increase. A similar behavior occurs when entering in the  $S = 2$  region ( $J=K = 0.6$ ) but now the maximum of  $\chi(q)$  is located at  $q = (4; 5; 0)$  corresponding to the IC order. This behavior does not depend qualitatively on other choices of the set of reciprocal vectors entering in

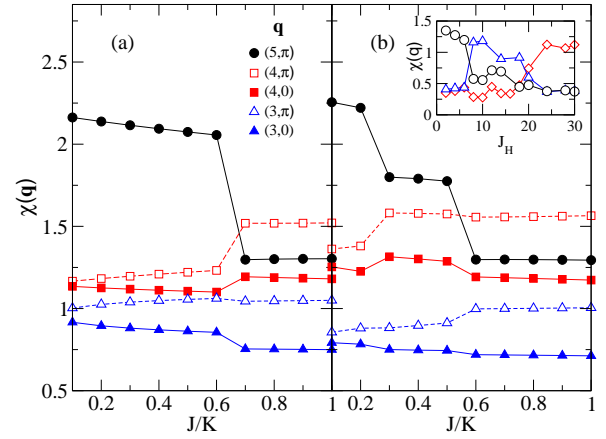


FIG. 5: (Color online) Static magnetic structure factor  $\chi(q)$  as a function of  $J$  along cuts of constant  $t$  on the phase diagrams of Fig. 3,  $2 \times 10$  cluster, 4 holes, (a)  $\nu_1 = 2$ ,  $t = 0.8$ , (b)  $\nu_1 = 1$ ,  $t = 0.2$ . The values of  $q$  are indicated on the plot,  $q_k$  in units of  $\pi/5$ . The inset shows  $\chi(q)$  for the ferromagnetic Kondo lattice model as a function of  $J_H$ ,  $L = 10$ ,  $n = 0.6$ ,  $q_x = 3$  (circles),  $2$  (triangles) and  $1$  (diamonds) in units of  $\pi/5$ .

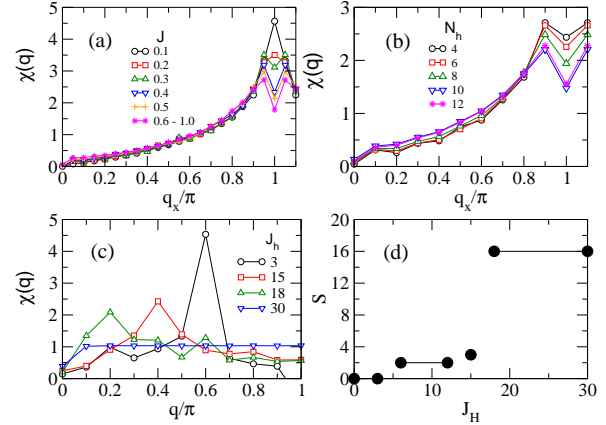


FIG. 6: (Color online) Static magnetic structure factor  $\chi(q)$  computed with DMRG (a) in the  $2 \times 40$  cluster, for several values of  $J$  indicated on the plot,  $\nu_1 = 1$ , and  $t = 0.3$ ; (b) in the  $2 \times 20$  cluster for  $\nu_1 = 1$ ,  $t = 0.4$ ,  $J = 1$  at several hole doping  $N_h$  indicated on the plot; (c) for the FKL model in the  $L = 20$  chain,  $x = 0.6$ , for several  $J_H$  indicated on the plot. (d) Total spin of the ground state of the FKL model as a function of  $J_H$ ,  $L = 20$ ,  $x = 0.6$ .

the Fourier transform. The inset shows  $\chi(q)$  for localized spins for the FKL model as a function of  $J_H$  for the same chain length,  $L = 10$ , and filling  $n = 0.6$ . In this case,  $q$  is reduced from  $3\pi/5$  to its minimum possible nonzero value,  $\pi/5$ , which corresponds to FM order in the  $S^z = 0$  subspace with PBC. It is clear the presence of two crossovers, at  $J_H = 6.5$  and at  $19.5$ , where also the total spin of the system jumps from  $0$  to  $1$  and then from  $1$  to  $2$ , respectively.



Similar behavior of the static magnetic structure factor is observed in the  $2 \times 20$  and  $2 \times 40$  clusters with OBC. Fig. 6(a) shows  $\langle q \rangle$  in the  $2 \times 40$  as a function of  $q$  for various values of  $J$ , at  $t = 0.3$ , obtained with DMRG. In this case only the spins of the spin chain have been included in the Fourier transform but results involving all spin-spin correlations are similar. It can be seen that, for a fixed  $t$ ,  $\langle q \rangle$  remains approximately unchanged during some intervals of  $J$ . Each of these intervals of  $J$  can be related to a given value of the total spin  $S$ , but there is not necessarily a one-to-one correspondence. As hole doping increases, the IC peak of  $\langle q \rangle$  becomes sharper but it remains at  $q = (\pi/2, 0)$ , as it can be seen in Fig. 6(b). We will term these states with  $S > 0$  as IC ferrimagnetic states. This behavior, which was also observed for the other clusters studied, is different from the one reported for the 1D FKL model.<sup>13</sup> In the FKL model, when the electron occupation is reduced from half-filling at a fixed value of the Hund coupling, the peak of the static magnetic structure factor, located at  $2k_F = \pi$ , is reduced from its AF value  $q_k = \pi$  to  $q_k = 0$  in the FM region. In Fig. 6(c) we show for comparison the evolution of  $\langle q \rangle$  for the FKL model as  $J_H$  is increased at an equivalent cluster size and filling. In contrast with Fig. 6(a), the peak of  $\langle q \rangle$  moves away from its IC position as it approaches the crossover to the FM phase located at  $J_H \approx 18$ . Inside this phase,  $\langle q \rangle$  presents the typical form of a FM order in the  $S^z = 0$  subspace. In Fig. 6(d) we show the corresponding evolution of the total spin of the ground state. Although DMRG calculations have a very slow convergence for this model, a problem that is also present in Lanczos diagonalization, there are apparently regions in  $J_H$  with intermediate values of  $S$  which may correspond to the various positions of the peak of  $\langle q \rangle$  shown in Fig. 6(c). However, this staircase in the values of  $S$  is not as pronounced as the one for model (1). Moreover, these results could be affected by finite size effects. These differences between the two models illustrate the IC ferrimagnetic character of the ground state in the present model as opposed to the true ferrimagnetic state present in the FKL model.

#### IV. TRANSPORT PROPERTIES

For the possible applications of  $\text{VO}_x$  in spintronics devices, it is essential to determine the correlation between its magnetic and transport properties. That is, one would expect that, as in manganites, transport is enhanced as the total spin of the ground state increases.

An elementary indication of charge mobility is provided by the kinetic energy,  $E_K$ . Fig. 7(a) and (b) show  $E_K$  obtained by ED for the  $2 \times 10$  cluster with 4 holes in the  $S^z = 0$  sector for  $\nu = 2$  and  $\nu = 1$  respectively. It can be seen in Fig. 7 that as  $J$  is increased for a fixed  $t$  there are step-like reductions of  $E_K$  at values of  $J$  which exactly coincide with the boundaries between regions with increasing values of  $S$  in the phase diagram

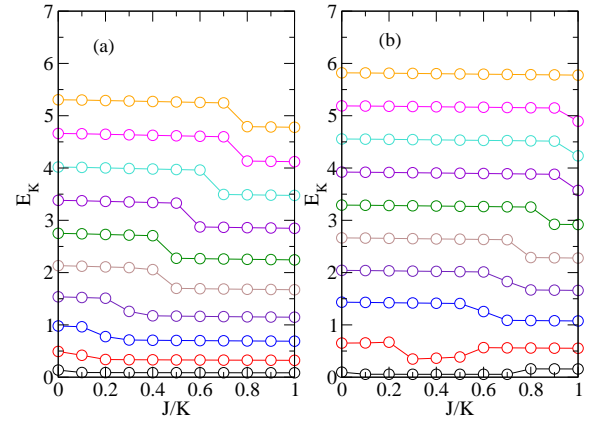


FIG. 7: (Color online) Kinetic energy (in units of  $K$ ) as a function of  $J$  on the  $2 \times 10$  cluster with 4 holes,  $t = 0.1; 0.2; \dots; 1.0$  from bottom to top (a)  $\nu = 2$ , (b)  $\nu = 1$ .

shown in Fig. 3. That is, the increase of  $S$  is accompanied by an increased hole localization. Although it is not perceptible in the scale of Fig. 7, in addition to these steps,  $E_K$  slowly decreases as  $J$  is increased due to the competing magnetic energy.

For small values of the hopping constant  $t$  ( $t \ll 0.2$ ), small increases of  $E_K$  as a function of  $J$  can also be observed in Fig. 7(b). This behavior can be understood from the fact that in the regime  $t \ll K$ , in order to gain magnetic energy, the spins on the  $t$ - $J$  chain have the tendency to form hole-free islands thus leading to a phase separated state. The exchange couplings  $J_1$  and  $J_2$  connecting the  $t$ - $J$  chain with the Heisenberg chain are competing with  $K$  and then opposite to the formation of those islands. Then, as  $J_1 = J_2 = J$  increase there will be at some point a breaking of that phase separated state thus favoring hole delocalization and an increase in kinetic energy.

A similar behavior of the kinetic energy has been observed in the  $2 \times 20$  cluster with 8 holes, and for the  $2 \times 40$  cluster with 16 holes as shown in Fig. 8(a) and (b) respectively. In order to clearly appreciate the evolution of  $E_K$  for various values of  $t$ , the values of  $E_K$  have been shifted by multiples of  $t$  as indicated in the vertical axis. For a given value of  $t$  there is a general decrease of  $E_K$  as  $J$  increases, with some sudden drops which coincide with the successive increases of  $S$  shown in the phase diagram of Fig. 4. It can be seen in the inset of Fig. 8 that the kinetic energy per doped hole also decreases as hole doping is increased. In the FKL model,  $E_K$  also decreases as  $J_H$  increases at a given density<sup>12</sup> due again to the competition with the magnetic energy (see further discussion below) but  $E_K$  per electron increases for a fixed  $J_H$ .

Fig. 9 shows the regular part of the optical conductivity  $\sigma^{reg}(\omega)$  computed on the  $2 \times 10$  cluster with 4 holes, (a)  $t = 0.4$ , (b)  $t = 0.9$ ,  $\nu = 1$ . Excluding the peak at  $\omega = 0$  which should be replaced by the Drude weight,<sup>18</sup>  $\sigma^{reg}(\omega)$  and  $\chi''(\omega)$  coincide, so we will use  $\chi''(\omega)$  in the following. For both values of  $t$ ,  $\chi''(\omega)$  presents a broad

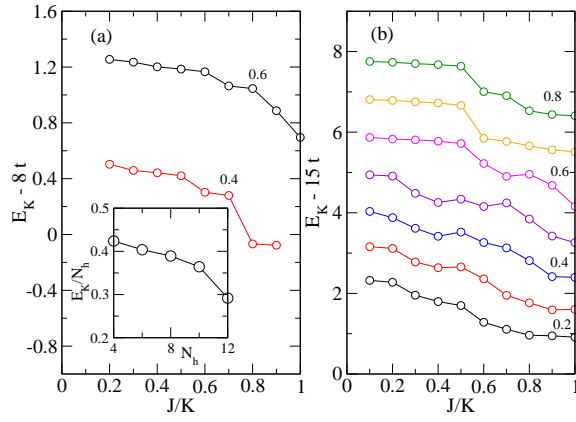


FIG. 8: (Color online) Kinetic energy  $E_K$  (in units of  $K$ ) as a function of  $J$ , for several values of  $t$  indicated on the plot,  $\mu_1 = 1$ , (a) for the  $2 \times 20$  cluster with 8 holes, (b) for the  $2 \times 40$  cluster with 16 holes.  $E_K$  has been shifted as indicated in the label of the y axis for clarity. The inset shows  $E_K$  per hole in the  $2 \times 20$  cluster as a function of the number of holes.

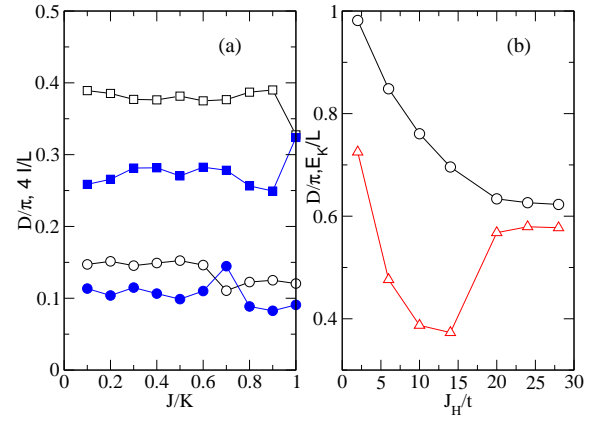


FIG. 10: (Color online) (a) D nude weight (open symbols) and the integral of  $\sigma^{reg}(\omega)$  (full symbols) for model (1) for the  $2 \times 10$  cluster with 4 holes,  $\mu_1 = 1$ , as a function of  $J$ ,  $t = 0.4$  (circles) and  $t = 0.9$  (squares). (b) D nude weight (triangles) and kinetic energy per site (circles) for the FKL model for  $L = 10$  cluster, 6 conduction electrons, as a function of  $J_H/t$ .

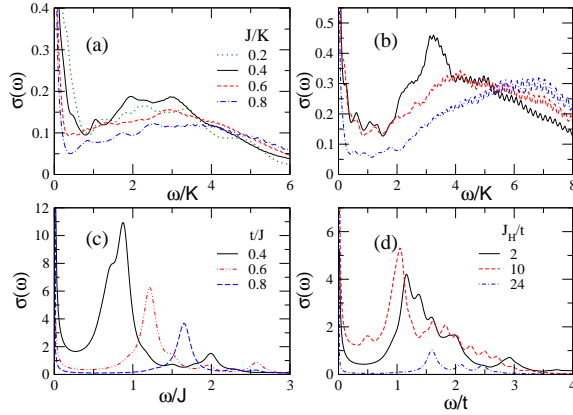


FIG. 9: (Color online) Optical conductivity (in units of  $e^2$ ) for the  $2 \times 10$  cluster with 4 holes,  $\mu_1 = 1$ , (a)  $t = 0.4$ , (b)  $t = 0.9$ , and for several values of  $J$  indicated in the plot. (c) Optical conductivity for the 1D extended  $t$ - $J$  model on the 10-site chain,  $J = 1$ ,  $\mu_1 = 1$ , 4 holes, and several values of  $t/J$  as indicated in the plot. (d) Optical conductivity for the FKL model (Eq. 5) on the 10-site chain, 6 conduction electrons, and several values of  $J_H/t$  indicated on the plot.

maximum starting at  $4t$ . For a fixed  $t$ , this maximum first increases as  $J$  is increased from 0.2 to 0.4, and then it decreases as  $J$  is further increased. The position of this maximum is shifted to higher values of  $\omega$ . In Fig. 9(c),  $\sigma(\omega)$  is shown for the 1D  $t$ - $J$  model, on the 10-site chain with 4 holes. Notice that  $J$  is actually  $K$  in the notation of the Hamiltonian (1) and hence we adopted the value  $J = 1$ . Also, for the sake of comparison, an on-site potential every two sites, with  $\mu_1 = 1$ , was added to the usual  $t$ - $J$  Hamiltonian. The behavior of  $\sigma(\omega)$  in both models is clearly different. In the extended  $t$ - $J$  model there is a peak located at  $\omega = 2t$  instead of the broad feature

observed for the FTJM model. In the present model,  $\sigma(\omega)$  is more resemblant to the behavior in two-dimensional clusters.<sup>18</sup> In two dimensions, the competition between kinetic and magnetic energies is more important than in one dimension, where in general spin-charge separation holds.  $\sigma(\omega)$  for the FTJM model is also more similar to the one for the FKL model (5), as shown in Fig. 9(d) for an equivalent chain size and filling: the incoherent structure is broad, and the spectral weight below this region (but at finite  $\omega$ ) may correspond in both models to the presence of a pseudogap. However, in the FKL model there is a pronounced change of  $\sigma(\omega)$  when entering in the FM region ( $J_H/t = 19$ ) implying an important transfer of weight from the incoherent part to the D nude peak. This behavior in the FM region is consistent with that reported in previous studies,<sup>20,23,24</sup> and it has been understood within the DE model.<sup>26</sup> The small remaining incoherent part does not scale with  $J_H/t$  and it is almost certainly a finite size effect. This suppression of the incoherent part of  $\sigma(\omega)$  is virtually absent in the frustrated  $t$ - $J$  model for VOx. Notice also the much smaller scale of  $\sigma(\omega)$  for the FTJM model with respect to those for the extended  $t$ - $J$  and FKL models. These different scales are in part due to the fact that  $t$  was used as the scale of energy in the latter models while  $K$  was used in our model. However, even after correcting for this factor, there is still an order of magnitude between  $\sigma^{reg}(\omega)$  in the FTJM model and the other two models.

Finally, the D nude weight for the  $2 \times 10$  cluster with 4 holes,  $\mu_1 = 1$ , is shown in Fig. 10(a) as a function of  $J$ , for  $t = 0.4$  and  $t = 0.9$ . It is instructive to examine first the behavior of the integral  $I$  of  $\sigma^{reg}(\omega)$  (second term in Eq. (4)) which measures the weight of the incoherent part of the optical conductivity. This quantity, for a given value of  $t$ , presents a maximum just at the crossover be-

tween the  $S = 0$  and  $S > 0$  phases, and then it smoothly decreases upon further increase of  $J$ . However, this integral is much smaller than the kinetic energy (notice the factor of 4 in Fig. 10). As a result, as it can be clearly seen in this Figure, the Druce weight qualitatively follows the behavior of the kinetic energy, shown in Fig. 7(b). That is, for a given value of  $t$  it presents sudden drops at the values of  $J$  at which the total spin of the ground state increases. The behavior of the Druce weight of model (1) is quite different from that of the FKL model. In Fig. 10(b) we show the Druce weight for the later model on the  $L = 10$  chain with PBC, 6 conduction electrons, obtained by ED. Although the kinetic energy monotonically decreases when  $J_H = t$  increases due to the competition with the magnetic energy<sup>12</sup>, the Druce weight first decreases while still inside the IC phase and then it is strongly enhanced upon entering in the FM phase, approximately at  $J_H = t = 19$ , as mentioned above. This sudden increase of the Druce weight is consistent with the noticeable suppression of the incoherent structure of the optical conductivity in the FM region, observed in Fig. 9(d).

## V. CONCLUSIONS

We have proposed a 1D model to describe a mechanism suggested to explain the appearance of a FM phase in vanadate nanotubes upon doping. This model consists of a  $t$ - $J$  chain coupled to a Heisenberg chain with frustrated exchange interactions.

Magnetic properties show the presence of an ascending "staircase" of the total spin  $S$  as the magnetic couplings  $J_1 = J_2 = J$  increase for a fixed value of the hopping integral  $t$ . These phases with  $S > 0$  have a ferrimagnetic origin and spin-spin correlations do not present the typical behavior of a ferromagnetic state but they correspond to an incommensurate phase which is described by a peak of the structure magnetic factor located at  $q = ((L-1)/L; 0)$  independently of the doping fraction. Our results suggest that this ferrimagnetic phase will survive in the thermodynamic limit. We have also observed

this staircase in  $S$  in the FKL model, a result which was not reported to our knowledge in previous studies on this model.<sup>13,15,16</sup> However, we cannot exclude at this point the possibility of this result being a mere finite size effect. In this model, we have also observed that the magnetic peak moves from its IC value to its FM value in a step-like fashion as  $J_H = t$  increases at a fixed density.

The optical conductivity for the 1D model for  $\text{VO}_x$  shows a broad incoherent structure with indications of the presence of a pseudogap, and spectral weight that is transferred to higher frequencies as  $J$  is increased for a given value of the hopping constant  $t$ . This behavior is different from the one observed in isolated  $t$ - $J$  chains, and more relevant to the topic of ferromagnetic metals, it is also very different from the one observed in the 1D FKL model. This different behavior in  $\sigma(\omega)$  is translated to the Druce weight. In the FKL model there is a strong enhancement of the Druce weight upon entering in the FM phase, while in the present model the Druce weight essentially follows the behavior of the kinetic energy.

In summary, in the proposed model for  $\text{VO}_x$ , at least in its 1D version, there is not a true ferromagnetic order but rather an IC ferrimagnetic one, and contrary to what happens in the FKL model, electronic transport is somewhat suppressed by this ferrimagnetic order. More realistic variants of the model here studied would include a three-chain ladder or a two-dimensional lattice, a Hubbard interaction instead of the  $t$ - $J$  one, and a dimerization on the  $t$ - $J$  chain. By increasing the dimensionality it could be possible to achieve a ratio between  $V_1, V_2$  and  $V_3$  ions closer to the real system. It would be closer to the actual materials to include a direct hopping between  $V_2$  sites. Even for the present model, we have only explored a small region in the parameter space, and in particular it seems promising to examine the case  $J_1 \neq J_2$ , as we plan to perform in future works.

## Acknowledgments

We thank A. Dobry, C. Gazza, G. B. Martins, M. E. Torio and S. Yunoki for useful discussions.

<sup>1</sup> S. A. Wolf, D. D. Awschalom, R. A. Buhrman, J. M. Daughton, S. von Molnar, M. L. Roukes, A. Y. Chtchelkanova, and D. M. Treger, *Science* 294, 1488 (2001). S. Maekawa and T. Shinjo, *Spin Dependent Transport in Magnetic Nanostructures*. (Taylor & Francis, London, 2002).

<sup>2</sup> M. B. Salamon and M. Jaime, *Rev. Mod. Phys.* 73, 583 (2001); J. M. D. Coey, M. Viret, and S. von Molnar, *Adv. Phys.* 46, 7268 (1992); T. Kaplan and S. Mahanti, (eds.), *Physics of Manganites*, (Kluwer Academic/Plenum Publishers, New York, 1999).

<sup>3</sup> A. P. Ramirez, *J. Phys.: Condens. Matter* 9, 8171 (1997), and references therein.

<sup>4</sup> L. K. Rusin-Ebba, D. M. News, H. Zeng, V. Derycke, J. Z. Sun, and R. Sandstrom, *Nature* 431, 672 (2004).

<sup>5</sup> P. Levy, A. G. Leyva, H. E. Troiani, and R. D. Sanchez, *Appl. Phys. Lett.* 83, 5247 (2003); J. Curiale, R. D. Sanchez, H. E. Troiani, A. G. Leyva, and P. Levy, *Appl. Phys. Lett.* 87, 043113 (2005).

<sup>6</sup> A. N. Pasupathy, R. C. Bialczak, J. Martinek, J. E. Grose, L. A. K. Donev, P. L. McEuen, and D. C. Ralph, *Science* 306, 86 (2004).

<sup>7</sup> J. Martinek, M. Sindel, L. Borda, J. Bamas, J. Konig, G. Schon, and J. von Delft, *Phys. Rev. Lett.* 91, 247202 (2003); C. J. Gazza, M. E. Torio, and J. A. Riera, *Phys. Rev. B* 73, 193108 (2006).



- <sup>8</sup> E. Vavilova, I. Hellmann, V. Kataev, C. Taschner, B. Buchner, and R. Klingeler, *Phys. Rev. B* **73**, 144417 (2006).
- <sup>9</sup> F. Krumreich, H.-J. Mühr, M. Niederberger, F. Bieri, B. Schwyder, and R. Nesper, *J. Am. Chem. Soc.* **121**, 8324 (1999).
- <sup>10</sup> X. Liu, C. Taschner, A. Leonhardt, M. H. Rummeli, T. Pichler, T. Gemming, B. Buchner, and M. Knupfer, *Phys. Rev. B* **72**, 115407 (2005).
- <sup>11</sup> S. J. Tans, A. R. M. Verschueren, C. Dekker, *Nature* **393**, 49 (1998); K. Tsukagoshi, B. W. Alphenaar, H. Ago, *Nature* **401**, 572 (1999); M. J. Biercuk, S. Garaj, N. Mason, J. M. Chow, C. M. Marcus, *Nano Letters* **5**, 1267 (2005).
- <sup>12</sup> J. Riera, K. Hallberg and E. Dagotto, *Phys. Rev. Lett.* **79**, 713 (1997).
- <sup>13</sup> E. Dagotto, S. Yunoki, A. L. Malvezzi, A. Moreo, J. Hu, S. Capponi, D. Poilblanc, and N. Furukawa, *Phys. Rev. B* **58**, 6414 (1998).
- <sup>14</sup> T. Hotta, M. Moraghebi, A. Feiguin, A. Moreo, S. Yunoki, and E. Dagotto, *Phys. Rev. Lett.* **90**, 247203 (2003).
- <sup>15</sup> D. J. Garcia, K. Hallberg, B. A. Lascio, and M. Avignon, *Phys. Rev. Lett.* **93**, 177204 (2004).
- <sup>16</sup> J. Kienert and W. Nolting, *Phys. Rev. B* **73**, 224405 (2006).
- <sup>17</sup> *Density-Matrix Renormalization*, edited by I. Peschel, X. Wang, M. Kaulke, and K. Hallberg, (Springer, Berlin, 1999); U. Schollwöck, *Rev. Mod. Phys.* **77**, 259 (2005).
- <sup>18</sup> E. Dagotto, *Rev. Mod. Phys.* **66**, 763 (1994).
- <sup>19</sup> R. M. Fye, M. J. Martins, D. J. Scalapino, J. Wagner, and W. Hanke *Phys. Rev. B* **44**, 6909 (1991).
- <sup>20</sup> S. Yunoki and A. Moreo, *Phys. Rev. B* **58**, 6403 (1998).
- <sup>21</sup> D. J. Garcia, K. Hallberg, C. D. Batista, M. Avignon, and B. A. Lascio, *Phys. Rev. Lett.* **85**, 3720 (2000).
- <sup>22</sup> See, e.g., T. Schork, S. Blawid, and J.-i. Igarashi, *Phys. Rev. B* **59**, 9888 (1999).
- <sup>23</sup> K. Held and D. Vollhardt, *Phys. Rev. Lett.* **84**, 5168 (2000).
- <sup>24</sup> For a study of the no-double occupancy version of the FKL model see P. Horsch, J. Jaklic, and F. Mack, *Phys. Rev. B* **59**, 6217 (1999).
- <sup>25</sup> T. Hakobyan, J. H. Hetherington, and M. R. Roger, *Phys. Rev. B* **63**, 144433 (2001), and references therein.
- <sup>26</sup> N. Furukawa, *J. Phys. Soc. Jpn.* **64**, 3164 (1995).